Textile & Leather Review

ISSN 2623-6281| www.tlr-journal.com | 10.31881/TLR

Green Preparation of Near-Infrared-Excited Upconversion (UCNP) Invisible Patterns on Clothing and Leather

Hongying Guo, Shuzhen Liu, Xiaojia Zhao, Xuan Li, Zhengguang Zhang, Ninghao Niu, Yunyang Xiao

How to cite: Guo H, Liu S, Zhao X, Li X, Zhang Z, Niu N, Xiao Y. Green Preparation of Near-Infrared-Excited Upconversion (UCNP) Invisible Patterns on Clothing and Leather. Textile & Leather Review. 2025; 8:1124-1139. https://doi.org/10.31881/TLR.2025.1124

How to link: https://doi.org/10.31881/TLR.2025.1124

Published: 29 December 2025

Green Preparation of Near-Infrared-Excited Upconversion (UCNP) Invisible Patterns on Clothing and Leather

Hongying GUO[1,2,3,4*], Shuzhen LIU[1,2,3,4], Xiaojia ZHAO[1,2,3,4], Xuan LI[1], Zhengguang ZHANG[1], Ninghao NIU[1], Yunyang XIAO[1]

[1]College of Chemical Engineering and Materials, Handan University, Handan 056006, Hebei, China

[2]Hebei Key Laboratory of Heterocyclic Compounds, Handan University, Handan 056006, Hebei, China

[3]Technology Innovation Center of Nanosized Natural Products and New Materials of Hebei Province, Handan 056006, Hebei, China

[4]Hebei Center for New Inorganic Optoelectronic Nanomaterial Research, Handan University, Handan 056006, Hebei, China

*lghy-2008@163.com

Article

https://doi.org/10.31881/TLR.2025.1124

Received 17 September 2025; Accepted 17 October 2025; Published 29 December 2025

ABSTRACT

This study addresses the critical need for advanced anti-counterfeiting solutions in the textile industry by developing a sustainable functional finishing process. The methodology utilizes upconversion nanoparticles (UCNPs), which convert near-infrared (NIR) light into visible green emission, thereby providing a high-security, invisible anti-counterfeiting feature. An eco-friendly, water-based ink was formulated and successfully applied to cotton fabric using the industry-standard screen-printing technique. The process employs a low-temperature curing step (105 °C) to minimize thermal damage and preserve the inherent flexibility of the textile substrate. The finished fabric patterns remain completely invisible under ambient light but exhibit brilliant, characteristic green luminescence under 980 nm NIR excitation, which can be readily authenticated using digital imaging sensors, even under safe, low-power irradiation. Importantly for apparel applications, the patterns demonstrate outstanding durability. The finished cotton fabric retains over 85% of its initial luminescence after 10 standard washing cycles, indicating excellent washing fastness. Furthermore, superior dry and wet rubbing fastness ratings of Grade 4–5 were achieved. This work presents a scalable and environmentally friendly strategy for integrating high-security luminescent features into textiles, providing a practical solution for brand protection that aligns with the principles of sustainable textile manufacturing.

KEYWORDS

textile anti-counterfeiting, functional finishing, upconversion nanoparticles, screen printing, washing fastness

INTRODUCTION

The proliferation of counterfeit goods has become a formidable challenge for the global economy, with the apparel and luxury leather sectors among the most heavily targeted industries [1]. The Organization for Economic Co-operation and Development (OECD) reports that trade in counterfeit goods constitutes a multi-billion-dollar illicit industry, resulting in significant revenue losses and brand dilution for legitimate manufacturers, while deceiving consumers with products of inferior quality and questionable safety [2]. In response, brand protection strategies have evolved from simple overt features, such as logos and watermarks, to more sophisticated technologies [3]. First-generation security features included holograms and specialty inks (e.g., thermochromic or photochromic), which, while initially effective, were soon replicated by counterfeiters with increasing accuracy [4]. Second-generation solutions, such as RFID tags and QR codes, offer unique item-level identification but are susceptible to electronic cloning, hacking, or physical removal, and their integration can alter the product's aesthetic and tactile qualities [5,6]. This has propelled the search for third-generation security features, which are covert, deeply integrated into the material itself, and require specialized, non-trivial equipment for authentication [7,8].

Luminescent materials have emerged as a cornerstone of covert security technologies [9]. Traditional down-shifting materials, including organic fluorescent dyes and quantum dots (QDs), absorb high-energy light (typically in the UV range) and emit lower-energy visible light [10,11]. While widely used, these materials are plagued by significant drawbacks. Organic dyes suffer from poor photostability, often degrading rapidly upon prolonged exposure to light, and their broad emission spectra can be easily mimicked [12,13]. QDs, while offering sharper emissions and better stability, often contain heavy metals such as cadmium, raising environmental and health concerns. Furthermore, the reliance on UV excitation for both is problematic, as many natural and synthetic materials, including textiles and finishing agents, exhibit autofluorescence under UV light, resulting in a low signal-to-noise ratio and potentially false-positive readings [14].

In this context, lanthanide-doped upconversion nanoparticles (UCNPs) represent a paradigm shift in optical security materials. Their unique anti-Stokes emission process, wherein they absorb low-energy NIR light and convert it into higher-energy visible light, provides a suite of unparalleled advantages [15]. The excitation source, typically a 980 nm or 808 nm laser, falls within the biological "optical transparency window," where autofluorescence from substrates is virtually nonexistent [16]. This ensures an exceptionally high signal-to-noise ratio, allowing for unambiguous signal detection. NIR light also exhibits greater penetration depth into

materials compared to UV, enabling the detection of UCNPs embedded within a polymer matrix or even beneath a thin surface layer. Moreover, lanthanide-doped materials are exceptionally photostable and chemically inert, promising a long operational lifetime for the security feature [17].

Despite these compelling attributes, the transition of UCNPs from laboratory curiosities to industrially viable security features for textiles and leather has been slow, primarily due to processing challenges. The most efficient UCNPs are often synthesized via high-temperature co-precipitation in organic solvents, resulting in nanoparticles with hydrophobic surfaces (e.g., oleate-capped) [18]. Integrating these into a coating requires their dispersion in polymer matrices such as PMMA or epoxy resins, which must in turn be dissolved in volatile organic compounds (VOCs) like toluene, xylene, or chloroform [19]. The widespread industrial use of such solvent-based systems is becoming untenable due to their significant environmental footprint, health risks to workers, and increasingly stringent global regulations (e.g., REACH in Europe) [20]. Furthermore, applying these coatings to flexible substrates presents additional challenges. Textiles require coatings that do not compromise their inherent breathability, flexibility, and hand feel. Leather, as a sensitive natural material, can be irreversibly damaged by harsh solvents and the high-temperature curing (often >150 °C) required for many solvent-borne systems [21].

Therefore, the development of a “green” and substrate-compatible application methodology is the most critical hurdle to the widespread adoption of UCNP technology in the fashion industry. A truly green approach must satisfy several criteria: (1) utilization of water as the primary solvent, eliminating VOCs; (2) use of nanoparticles that are inherently water-dispersible or synthesized via aqueous routes; (3) formulation with environmentally benign binders; and (4) employment of low-energy curing processes compatible with sensitive substrates. While some previous studies have explored water-based UCNP inks, they often focus on a single substrate or fail to provide comprehensive durability assessments, which are crucial for products subjected to daily wear, washing, and abrasion. This study directly addresses this critical gap. We propose a holistic green strategy encompassing the one-pot aqueous synthesis of hydrophilic $NaYF_4$:Yb,Er UCNPs and their formulation into a novel, water-based polyurethane (WPU) ink. This single ink system is designed for versatile application on both cotton fabric and bovine leather via the industrially scalable screen-printing method, followed by a gentle, low-temperature curing regimen. Our research aims to demonstrate that this sustainable approach can produce stealth anti-counterfeiting patterns with luminescence and durability performance that meet the rigorous demands of the modern apparel and leather goods industries.

Accordingly, this study is guided by a central research question: Can a fully aqueous-based system, integrating hydrothermally synthesized upconversion nanoparticles with a water-based polyurethane binder, be formulated into a screen-printable ink that produces highly durable and covert anti-counterfeiting patterns on both porous textiles and non-porous leather substrates? By systematically addressing this question, this work aims to establish a practical and sustainable pathway for advanced textile security, bridging the gap between nanomaterial synthesis and real-world industrial application.

MATERIALS AND METHODS

Materials

Yttrium(III) chloride hexahydrate ($YCl_3·6H_2O$, 99.9%), ytterbium(III) chloride hexahydrate ($YbCl_3·6H_2O$, 99.9%), and erbium(III) chloride hexahydrate ($ErCl_3·6H_2O$, 99.9%) were purchased from Sigma-Aldrich. Sodium hydroxide (NaOH, ≥98%), ammonium fluoride (NH_4F, ≥98%), oleic acid (OA, 90%), and ethanol (≥99.5%) were obtained from Aladdin Industrial Corporation. A commercial anionic WPU dispersion (aliphatic, 35 wt% solid content, pH 7.5) was sourced from an industrial supplier. All chemicals were of analytical grade and used without further purification. Deionized (DI) water (18.2 MΩ·cm) was used throughout all experiments.

The substrates used were 100% plain-woven cotton fabric (120 g/m^2) and chrome-tanned bovine leather (thickness 1.2 mm, semi-aniline finished surface). Prior to use, the cotton fabric was scoured in an aqueous solution containing 2 g/L NaOH and 1 g/L anionic surfactant at 95 °C for 60 minutes to remove natural waxes and impurities, followed by rinsing with hot and cold water until a neutral pH was achieved, and then air-dried. The leather surface was wiped with an isopropanol–water (1:1 v/v) solution to remove any surface dust or oils and then air-dried.

Green Synthesis of Hydrophilic UCNPs

The hydrophilic $NaYF_4$:Yb,Er nanoparticles were synthesized using a modified one-pot hydrothermal method. In a typical procedure, a rare-earth chloride stock solution was prepared by dissolving $YCl_3·6H_2O$ (0.78 mmol), $YbCl_3·6H_2O$ (0.20 mmol), and $ErCl_3·6H_2O$ (0.02 mmol) in 15 mL of DI water in a 100 mL beaker. Subsequently, 10 mL of NaOH solution (2.0 M) and 5 mL of oleic acid were added to the solution under vigorous magnetic stirring (800 rpm), forming a stable emulsion. In this hydrothermal method, oleic acid temporarily functions as a capping agent to control the crystal growth and morphology of the nanoparticles, which is essential for

achieving high luminescent efficiency. After 30 minutes, 10 mL of NH_4F solution (4.0 M) was added dropwise over 5 minutes. The resulting mixture was stirred for another 30 minutes to ensure homogeneity before being transferred into a 50 mL Teflon-lined stainless steel autoclave. The autoclave was sealed, placed in a programmable oven, and heated to 180 °C for 12 hours. After the reaction, the autoclave was allowed to cool naturally to room temperature. The product was collected by centrifugation (8,000 rpm, 10 min). A critical purification step was then performed to ensure the final product was hydrophilic and suitable for a water-based system: the nanoparticles were thoroughly washed three times with ethanol and DI water alternately. This step was designed to completely remove unreacted reagents and, most importantly, to modify the nanoparticle surface by displacing a significant portion of the hydrophobic oleic acid capping agent, rendering the UCNPs readily dispersible in the subsequent aqueous ink system. Finally, the purified hydrophilic UCNP powder was dried in a vacuum oven (60 °C, 12 h). The final product was a fine, white powder. The subsequent successful formulation of a stable aqueous ink (detailed in Section 2.3) demonstrated that the purification process was effective in rendering the nanoparticles readily dispersible in water.

Preparation of Green UCNP Ink

The eco-friendly UCNP ink was formulated by dispersing the as-prepared UCNP powder into the WPU binder. First, 1.0 g of UCNP powder was pre-dispersed in 11.0 mL of DI water. To ensure deagglomeration, this suspension was sonicated using an ultrasonic probe (20 kHz, 400 W) for 15 minutes in an ice bath to prevent overheating. This pre-dispersion was then added dropwise to 28.5 g of the WPU emulsion (containing 10.0 g of solid polyurethane) under constant mechanical stirring (500 rpm). This corresponds to a UCNP loading of 10% by weight relative to the solid content of the polyurethane binder (1.0 g UCNPs to 10.0 g solid WPU). The mixture was stirred for an additional 2 hours to ensure a homogeneous dispersion. The final ink had a solid content of approximately 27% and a viscosity suitable for screen printing. The rheological properties of the ink were measured using a rotational viscometer (Brookfield DV2T) with a cone-plate geometry at 25 °C.

Application of Stealth Patterns

UCNP stealth patterns were applied using a manual screen-printing process. A polyester screen with a mesh count of 120 threads per inch, tensioned on an aluminum frame, was used. A star-shaped pattern (3 cm in diameter) was created on the screen using a water-resistant photo-emulsion. The substrate (cotton or leather) was placed on a flat vacuum printing table. A small amount of the UCNP ink was placed along one edge of

the pattern. A 70-durometer polyurethane squeegee was used to draw the ink across the screen at a 75° angle with firm, consistent pressure. This action forced the ink through the open mesh of the pattern onto the substrate. After printing, the samples were pre-dried in an oven at 80 °C for 5 minutes to evaporate the bulk of the water, followed by a final curing step at 105 °C for 3 minutes. The curing condition (105 °C, 3 min) was established as a rapid "flash-curing" process. While this temperature nominally exceeds the shrinkage threshold of vegetable-tanned leathers, the chrome-tanned bovine substrate used in this study possesses significantly higher hydrothermal stability (typically T_s > 100 °C) due to robust chromium-collagen crosslinking. Crucially, the short duration ensures that thermal energy is primarily localized at the surface for ink film coalescence, minimizing heat transfer to the bulk collagen fibers. The safety of this protocol was quantitatively validated via thermal analysis (see Section 3.2).

The printed samples were conditioned at 23 ± 2 °C and 50 ± 5% relative humidity for 24 hours before characterization.

Characterization and Durability Testing

The crystal structure and optical properties of the UCNPs were characterized. To investigate the surface modification mechanism, Fourier transform infrared (FT-IR) spectra were recorded on a Nicolet iS50 spectrometer in the range of 4,000–400 cm^{-1} using the KBr pellet technique. The surface wettability of the nanoparticles before and after washing was evaluated by measuring the static water contact angle (WCA) on pressed nanoparticle disks using a goniometer (Krüss DSA25). Additionally, the colloidal stability and surface charge of the purified UCNPs in aqueous suspension were determined by zeta potential measurements using a Malvern Zetasizer Nano ZS at 25 °C. X-ray diffraction (XRD) patterns were collected on a Bruker D8 Advance diffractometer with Cu Kα radiation (λ = 1.5406 Å) over a 2θ range of 10–80°. The upconversion photoluminescence (PL) spectra were recorded on an Edinburgh Instruments FLS980 fluorescence spectrophotometer. A 980 nm fiber-coupled continuous-wave laser diode was used as the excitation source. For all measurements, the laser power was fixed at 200 mW, focused to a spot diameter of approximately 2 mm (corresponding to a power density of ≈6.4 W/cm^2), and the spectra were collected with an integration time of 1.0 s. To further elucidate the luminescence stability mechanism, fluorescence lifetime decay curves were recorded at the main emission peak (545 nm) using a time-correlated single-photon counting (TCSPC) technique with pulsed 980 nm laser excitation. The decay curves were fitted with a double-exponential function to calculate the average lifetime. It should be noted that the spectral data presented are the raw

data as recorded by the instrument, without any subsequent smoothing, filtering, or normalization routines applied. All spectra were recorded under these identical conditions to ensure comparability.

The surface morphology of the printed patterns on cotton and leather was examined with a scanning electron microscope (SEM; Hitachi SU8010) after sputter-coating the samples with a thin layer of gold. The optical transparency of a cured UCNP–WPU film cast on a quartz slide was measured using a UV–Vis spectrophotometer (Shimadzu UV-2600).

Durability was assessed through standardized tests. Washing fastness of the printed cotton was evaluated according to ISO 105-C06 (A1S). Samples were washed for 1, 3, 5, 7, and 10 cycles, with luminescent intensity measured after each interval. Abrasion resistance of the printed leather was tested using a Martindale abrasion tester (ISO 12947-1) under a 9 kPa load. The luminescence was measured at 0, 1,000, 2,500, and 5,000 cycles. Rubbing fastness for both substrates was determined according to ISO 105-X12 using a crockmeter, and the staining on the testing cloth was rated against the standard gray scale (1–5, where 5 is no color transfer).

RESULTS AND DISCUSSION

The overarching goal of this research was to engineer a green, yet highly effective, system for applying covert UCNP patterns onto textile and leather substrates. The success of this endeavor hinged on multi-stage validation: first, the synthesis of high-quality, water-dispersible nanoparticles; second, the formulation of a stable, eco-friendly, and processable ink; and third, the confirmation that the final printed patterns possess the desired stealth characteristics and can withstand the rigors of practical use.

Characterization of Synthesized UCNPs

The fundamental performance of the final security feature is intrinsically linked to the quality of the core luminescent material.

XRD analysis was performed to verify the crystal phase, a critical factor for luminescent efficiency. The diffraction pattern, shown in Figure 1a, exhibits sharp peaks located at 2θ values of 17.1°, 29.8°, 30.7°, 42.5°, and 52.8°. These peaks correspond to the (100), (110), (101), (201), and (300) crystal planes of the pure hexagonal β-$NaYF_4$ phase (JCPDS No. 16-0334). The absence of any peaks corresponding to the cubic (α) phase or other impurities signifies the successful synthesis of the high-efficiency hexagonal structure, which acts as an ideal host lattice for the Yb^{3+} sensitizer and Er^{3+} activator ions.

The optical properties are the most critical aspect of the UCNPs. Under continuous-wave 980 nm laser excitation, the nanoparticle powder exhibited bright, visible green light. The recorded photoluminescence spectrum (Figure 1b) confirms this observation quantitatively. It is dominated by two sharp emission bands, a strong peak centered at 545 nm and a shoulder peak at 525 nm. These emissions are the well-known electronic transitions of the erbium ion (Er^{3+}), corresponding to the $^4S_{3/2} \rightarrow {}^4I_{15/2}$ and $^2H_{11/2} \rightarrow {}^4I_{15/2}$ transitions, respectively. The mechanism involves the Yb^{3+} ions acting as sensitizers, efficiently absorbing the 980 nm photons and sequentially transferring the energy to neighboring Er^{3+} activator ions, which are then promoted to higher energy states before relaxing radiatively to the ground state, emitting higher-energy visible photons. The distinct and sharp emission signature is difficult to replicate with conventional pigments or dyes, forming the basis of its anti-counterfeiting capability. To verify the effectiveness of the green washing strategy, FT-IR analysis was conducted. As shown in Figure 1c, the as-synthesized nanoparticles (before washing) exhibited strong absorption peaks at 2,924 cm^{-1} and 2,853 cm^{-1}, corresponding to the asymmetric and symmetric stretching vibrations of the methylene ($–CH_2–$) groups in the long alkyl chain of the oleate ligands. However, after the sequential ethanol/water washing process, the intensity of these characteristic peaks significantly diminished. This reduction indicates that the physically adsorbed oleic acid layers and the bulk of the loosely bound capping agents were successfully removed, exposing the underlying surface for interaction with the aqueous medium.

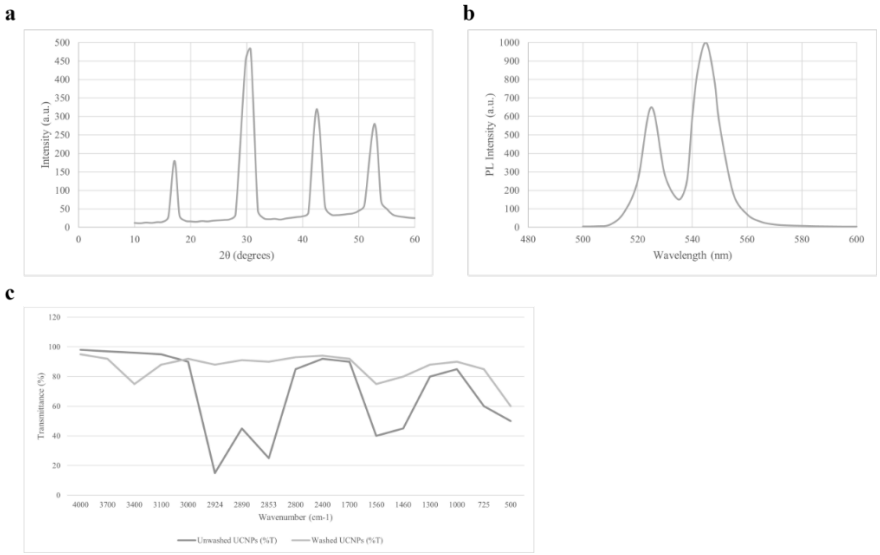

Figure 1. Crystallographic and optical characterization of as-synthesized NaYF4:Yb,Er upconversion nanoparticles (UCNPs). (a) X-ray diffraction (XRD) pattern of the UCNPs; (b) Upconversion photoluminescence (PL) spectrum under 980 nm laser excitation; (c) FT-IR spectra of the as-synthesized oleate-capped UCNPs and the purified hydrophilic UCNPs after the sequential washing process

The transformation in surface polarity was visually confirmed by WCA measurements. The unwashed nanoparticle disk displayed hydrophobicity with a WCA of approximately 108°, preventing water droplet spreading. In stark contrast, the washed UCNP disk exhibited excellent hydrophilicity, with the water droplet spreading immediately to form a contact angle of 32°. This result provides direct evidence that the washing treatment effectively reversed the surface properties from hydrophobic to hydrophilic.

Crucially, the colloidal stability mechanism was elucidated via zeta potential analysis. The purified UCNPs dispersed in neutral water (pH 7.0) exhibited a distinct positive surface charge with a zeta potential of +34.5 mV. This relatively high magnitude suggests that the removal of the oleate ligands exposed the positively charged lanthanide ions (Ln^{3+}) on the crystal surface. This induced strong electrostatic repulsion between the particles, preventing re-aggregation and ensuring long-term stability in the aqueous phase, even prior to the addition of the binder.

Ink Formulation and Pattern Characterization

A successful ink formulation requires more than just active particles; it must possess the right physical properties for application and form a robust film upon curing. The rheology of the 10% UCNP–WPU ink was analyzed. The ink exhibited shear-thinning behavior, with a viscosity of approximately 1,800 mPa·s at low shear rates, which dropped to approximately 450 mPa·s at higher shear rates. This non-Newtonian property is ideal for screen printing: the high viscosity at rest prevents the ink from dripping through the screen mesh, while the viscosity drop under the shear stress of the squeegee allows for smooth, easy transfer onto the substrate. While a more comprehensive rheological analysis, including thixotropic behavior, and a detailed study of the inks long-term storage stability were beyond the scope of this initial proof-of-concept work, the observed shear-thinning was sufficient to achieve consistent and high-quality prints for the subsequent durability assessments.

After printing and curing, the stealth and luminescent properties of the patterns were evaluated. Visually, the patterns were exceptionally covert. A cured film of the UCNP–WPU ink cast on a quartz slide appeared highly transparent to the naked eye. We acknowledge that a degree of light scattering is expected due to the refractive index mismatch between the UCNPs and the polymer matrix. Therefore, a more rigorous optical characterization, including film thickness and haze measurements, would be required for a quantitative assessment, which we propose as a subject for future investigation. On the white cotton, the pattern was

imperceptible, and on the black leather, it created only a very slight matte finish that was unnoticeable without close scrutiny. However, upon illumination with the 980 nm laser in a dimly lit room, the patterns became brilliantly luminous, emitting the characteristic green light. It is worth noting that the upconversion process is governed by a non-linear power dependence ($I \propto P^n$), meaning luminescence intensity drops significantly at lower excitation powers. While the patterns exhibit high brightness under the laboratory characterization power of 200 mW, practical application demands adherence to Class 1 eye-safety standards (<0.4 mW). Under such low-power regimes, the emission may fall below the naked-eye visibility threshold. However, this physical limitation is effectively addressed by the high photosensitivity of modern smartphone CMOS sensors. Unlike the human eye, digital sensors can integrate photon signals over time, allowing for clear capture and decoding of the security patterns even when excited by eye-safe, low-power laser sources. This renders the technology suitable for “covert-digital”authentication rather than simple visual inspection. The photoluminescence spectrum of the printed pattern was nearly identical to that of the original powder, indicating that the UCNPs were not damaged during ink formulation and curing, and that the WPU matrix is transparent to both the 980 nm excitation and the green emission.

The microstructure of the UCNP–WPU film on the substrates was visualized using SEM. On cotton fabric, the images showed that the ink did not merely sit on top of the fabric but penetrated the yarn structure, forming a thin, conformal sheath around the individual cotton fibers. This intimate fiber-level coating is critical as it binds the UCNPs securely without blocking the interstitial pores between yarns, which is expected to help maintain the fabric’s inherent flexibility and air permeability. While a quantitative analysis of changes to the leather’s softness or a colorimetric comparison was not performed, no visible discoloration, shrinkage, or stiffening of the leather was observed after the mild curing process. The uniform luminescence observed across the entire pattern strongly suggests that the individual UCNPs were well-dispersed within the polyurethane matrix in both cases, with no significant aggregation, which is key to achieving this optical performance. This critical surface modification yields a hydrophilic nanoparticle powder compatible with the eco-friendly, water-based polyurethane binder. To rigorously assess potential thermal damage to the leather substrate, differential scanning calorimetry (DSC) was performed. As shown in Figure 2, the denaturation temperature (T_d) of pristine leather was recorded at 112.5 °C. After the standard curing process (105 °C for 3 min), the leather exhibited a nearly identical endothermic peak centered at 111.8 °C. The negligible shift (ΔT < 1 °C) and preservation of peak enthalpy confirm that the bulk collagen fiber structure remained intact. This

is attributed to the short dwell time, which prevents the leather core from reaching the equilibrium temperature of the oven, thereby avoiding structural denaturation.

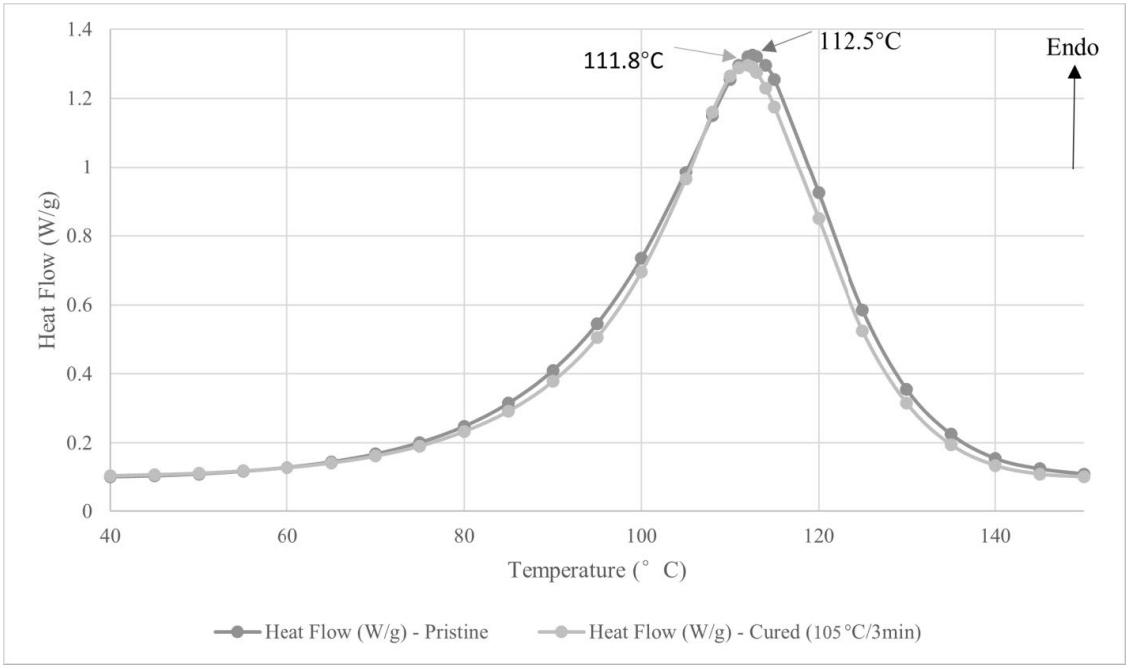

Figure 2. Thermal stability analysis of the leather substrate. Differential scanning calorimetry (DSC) curves of pristine chrome-tanned bovine leather (dark line) and leather after the curing process at 105 °C for 3 min (light-colored line). The minimal shift in the denaturation temperature peak (from 112.5 °C to 111.8 °C) and the preservation of the peak shape confirm that the rapid curing protocol did not cause significant thermal denaturation of the bulk collagen fiber structure

Durability and Fastness Performance

For any textile or leather application, durability is a non-negotiable prerequisite. The performance of the UCNP patterns was assessed through a series of rigorous, standardized tests, with the key results depicted graphically in Figure 3. The washing fastness test on cotton yielded highly encouraging results. As shown in Figure 3a, the relative luminescent intensity exhibited a gradual decline, retaining 86.4% of its initial value after 10 standard washing cycles. While this retention rate is considered excellent for functional textiles, the 13.6% loss warrants a deeper mechanistic investigation.

Typically, such reduction is attributed to the physical detachment of nanoparticles. However, this hypothesis contradicts our rubbing fastness results (Table 1), where the patterns achieved a Grade 4–5 in dry rubbing

and a Grade 4 in wet rubbing. These high ratings indicate that the UCNPs are firmly locked within the robust polyurethane matrix with negligible particle transfer. If physical detachment were the primary cause of the 13.6% intensity loss, a much lower rubbing grade would be expected.

To resolve this discrepancy, fluorescence lifetime analysis was performed (Figure 3c). The average lifetime (τ) of the pattern decreased from 485 μs (0 cycles) to 410 μs (10 cycles). This significant reduction indicates the occurrence of luminescence quenching, likely caused by water molecules penetrating the polymer matrix and interacting with the hydrophilic, shell-free nanoparticle surface. Consequently, the observed intensity decline is primarily optical (water-induced quenching) rather than mechanical (binder failure), further validating the exceptional physical robustness of the green UCNP–WPU ink.

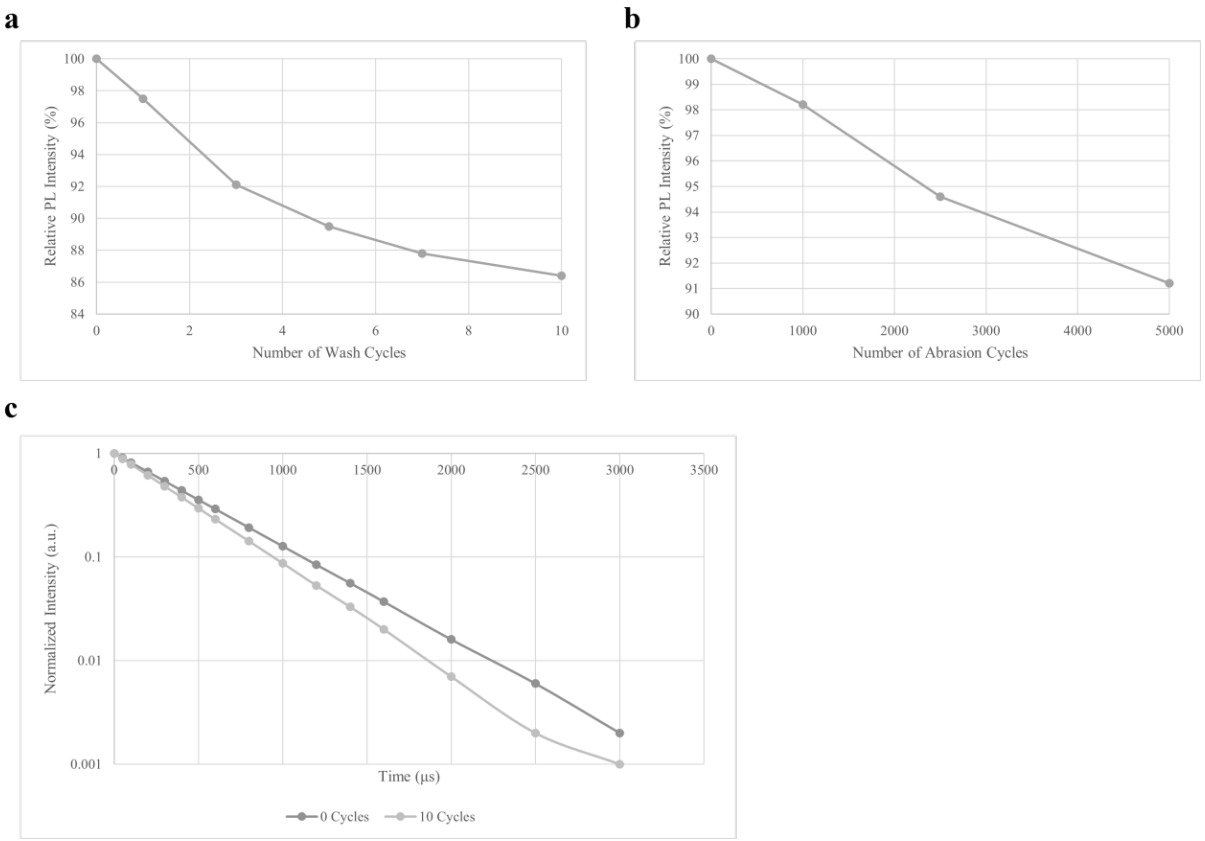

Figure 3. Durability assessment of the UCNP patterns on cotton and leather. (a) Relative photoluminescence (PL) intensity of the pattern on cotton fabric as a function of the number of wash cycles; (b) Relative PL intensity of the pattern on leather as a function of the number of abrasion cycles; (c) Fluorescence lifetime decay curves of the UCNP pattern on cotton before washing (0 cycles) and after 10 washing cycles (monitored at 545 nm under 980 nm excitation). The shortening of the lifetime indicates water-induced surface quenching

Collectively, these quantitative durability results provide strong evidence that our green preparation method produces patterns that are not only optically brilliant but also mechanically robust enough for real-world applications.

Table 1. Rubbing fastness results of UCNP patterns on cotton and leather according to ISO 105-X12

Substrate	Test Condition	Fastness Grade
Cotton Fabric	Dry Rubbing	4–5
Cotton Fabric	Wet Rubbing	4
Bovine Leather	Dry Rubbing	4–5
Bovine Leather	Wet Rubbing	4

Notes: Grades are based on the standard grey scale, where Grade 5 = no color transfer and Grade 1 = high color transfer.

CONCLUSION

In conclusion, this research establishes a robust, solvent-free processing strategy that demonstrates a water-based UCNP ink can be effectively utilized to fabricate covert security patterns with exceptional durability on both cotton and leather. Mechanistic analysis revealed that the ink system maintains superior mechanical stability (high rubbing fastness), confirming that the minor optical loss during washing is attributed to surface quenching by water molecules rather than physical particle detachment. The broader significance of this work lies in providing a viable and environmentally responsible blueprint for integrating advanced functional nanomaterials into sensitive, flexible substrates. By successfully eliminating toxic organic solvents and high-temperature curing, this methodology offers a practical engineering solution for brand protection in the fashion and luxury goods sectors, aligning with the principles of low-VOC manufacturing and energy efficiency. Looking forward, while this study has established a viable water-based processing pathway, the transition from laboratory prototype to commercial product requires addressing specific industrialization benchmarks. To ensure full life-cycle safety, future work should prioritize standard regulatory compliance assessments in

accordance with frameworks such as REACH, including comprehensive toxicological profiling and biocompatibility validation for consumer goods. With respect to commercialization, a critical trade-off exists between optical safety and visual brightness due to the non-linear nature of upconversion. Consequently, the practical roadmap for this technology should shift from "direct visual inspection" to "smartphone-assisted verification." Future work will focus on developing a dedicated mobile application that leverages the superior sensitivity of camera sensors to capture low-intensity patterns excited by Class 1 eye-safe lasers. This approach not only resolves the safety-visibility paradox but also integrates the anti-counterfeiting feature into the digital supply chain ecosystem. With these considerations in mind, this validated platform opens several promising avenues. A crucial next step would be to quantitatively benchmark the performance of this solvent-free system against traditional solvent-based inks to further validate its industrial superiority. Building upon this, the development of multi-color patterns using different lanthanide dopants (e.g., thulium for blue, holmium for red) could create higher-level encryption features. For ultimate permanence, future research could explore integrating these UCNPs directly into fibers during the spinning process. Finally, beyond anti-counterfeiting, the unique optical properties of UCNPs within a flexible, durable binder could be leveraged for developing next-generation smart textiles, such as wearable biochemical sensors or interactive thermochromic displays.

Availability of Data and Materials

The datasets used and/or analysed during the current study were available from the corresponding author on reasonable request.

Author Contributions

Hongying Guo and Xuan Li designed the study; all authors conducted the study; Xiaojia Zhao, Yunyang Xiao and Ninghao Niu collected and analyzed the data. Zhengguang Zhang and Shuzhen Liu participated in drafting the manuscript, and all authors contributed to critical revision of the manuscript for important intellectual content. All authors gave final approval of the version to be published. All authors participated fully in the work, took public responsibility for appropriate portions of the content, and agreed to be accountable for all aspects of the work in ensuring that questions related to the accuracy or completeness of any part of the work were appropriately investigated and resolved.

Funding

Handan Science and Technology Research and Development Program (Project No. 21422111172).

Conflict of Interest

The authors declare no conflict of interest.

Acknowledgments

Not applicable.

REFERENCES

[1] Trade I. Mapping Global Trade in Fakes. 2025. Available from: https://formatresearch.com/wp-content/uploads/2025/05/Mapping-Global-Trade-in-Fakes-2025.pdf. doi: 10.1787/g2g9f533-en

[2] Trade I. Trends in trade in counterfeit and pirated goods. Economic Cooperation and Development (OECD) and the EUIPO 2019 Report. 2019. Available from: https://www.oecd.org/content/dam/oecd/en/publications/reports/2019/03/trends-in-trade-in-counterfeit-and-pirated-goods_g1g9f533/g2g9f533-en.pdf. doi: 10.1787/g2g9f533-en

[3] Wilson JM. Brand protection and the global risk of product counterfeits: A total business solution approach. Cheltenham, England: Edward Elgar Publishing; 2022.

[4] Sezonov VS, Fialka MI, Poltavski EM, Prokopenko NM, Fomenko MV. Forensic Examination of Electronic Documents. Law, State & Telecommunications Review/Revista de Direito, Estado e Telecomunicações. 2022; 14(2). doi: 10.26512/lstr.v14i2.40965

[5] Gudymenko I, Hutter M. Security in the Internet of Things. Proceedings of Intensive Program on Information Communication Security (IPICS 2011). 2011: 22-31.

[6] Chevalier M, Gutsatz M. Luxury retail and digital management: Developing customer experience in a digital world. Hoboken, NJ, USA: John Wiley & Sons; 2020.

[7] Lindstrand M. Optical document security: Measurement, characterization and visualization: In the light of visual evaluation. Linköping, Sweden: Linköping University Electronic Press; 2019. doi: 10.3384/diss.diva-151626

[8] Syed MR. Multimedia Technologies: Concepts, Methodologies, Tools, and Applications: Concepts, Methodologies, Tools, and Applications. Hershey, PA, USA: IGI Global; 2008.

[9] Mondal PP, Neem M, Chand R, Pandit A, Neogi S. Luminescent metal–organic frameworks as multimodal platforms for advanced anticounterfeiting and security applications. Chemistry of Materials. 2024; 36(21):10451-10473. doi: 10.1021/acs.chemmater.4c01811

[10] Lakowicz J. Principles of Fluorescence Spectroscopy 3rd edition 2006; London, UK: Springer.

[11] Yang H-L, Bai L-F, Geng Z-R, Chen H, Xu L-T, Xie Y-C, et al. Carbon quantum dots: Preparation, optical properties, and biomedical applications. Materials Today Advances. 2023; 18:100376. doi: 10.1016/j.mtadv.2023.100376

[12] Abdou E, Hafez H, Bakir E, Abdel-Mottaleb M. Photostability of low cost dye-sensitized solar cells based on natural and synthetic dyes. Spectrochimica Acta Part A: Molecular and Biomolecular Spectroscopy. 2013; 115:202-207. doi: 10.1016/j.saa.2013.05.090

[13] Fu A, Gu W, Larabell C, Alivisatos AP. Semiconductor nanocrystals for biological imaging. Current Opinion in Neurobiology. 2005; 15(5):568-575. doi: 10.1016/j.conb.2005.08.004

[14] You M, Zhong J, Hong Y, Duan Z, Lin M, Xu F. Inkjet printing of upconversion nanoparticles for anti-counterfeit applications. Nanoscale. 2015; 7(10):4423-4431. doi: 10.1039/C4NR06944G

[15] Wang F, Liu X. Recent advances in the chemistry of lanthanide-doped upconversion nanocrystals. Chemical Society Reviews. 2009; 38(4):976-989. doi: 10.1039/B809132N

[16] Wang LV, Wu H-I. Biomedical optics: Principles and imaging. Hoboken, NJ, USA: John Wiley & Sons; 2007.

[17] Chaudhary B, Kshetri YK, Kim T-H. Photocatalysis, Anti-counterfeiting and Optical Thermometry Applications of Upconversion Nanoparticles. Upconversion Nanoparticles (UCNPs) for Functional Applications. London, UK: Springer; 2023. p. 193-220. doi: 10.1007/978-981-99-3913-8_8

[18] Kong W, Sun T, Chen B, Chen X, Ai F, Zhu X, et al. A general strategy for ligand exchange on upconversion nanoparticles. Inorganic Chemistry. 2017; 56(2):872-877. doi: 10.1021/acs.inorgchem.6b02479

[19] Hiemenz PC, Lodge TP. Polymer chemistry. Boca Raton, FL, USA: CRC Press; 2007. doi: 10.1201/9780429190810

[20] Agency EC. European Chemicals Agency (ECHA); London, UK: Elsevier; 2024.

[21] O'Flaherty F. The Chemistry and Technology of Leather. St. Louis, MO, USA: Reinhold; 1962.